

# Structural and Magnetic Properties of $\text{La}_{0.9}\text{Sr}_{0.1}\text{MnO}_3$ Micro and Nanometer-Sized Manganite Samples

Mahin Eshraghi<sup>1</sup> & Parviz Kameli<sup>2</sup>

<sup>1</sup> Department of physics, Payame Noor University, Tehran, Iran

<sup>2</sup> Department of physics, Isfahan University of Technology, Isfahan, Iran

Correspondence: Mahin Eshraghi, Department of physics, Payame Noor University, Tehran 19395-3697, Iran.  
Tel: 98-311-391-2375. E-mail: eshraghi@nj.isfpnu.ac.ir

Received: October 13, 2013 Accepted: November 26, 2013 Online Published: January 7, 2014

doi:10.5539/jmsr.v3n2p1 URL: <http://dx.doi.org/10.5539/jmsr.v3n2p1>

## Abstract

The structural and magnetic properties of micrometer and nanometer-sized samples of  $\text{La}_{0.9}\text{Sr}_{0.1}\text{MnO}_3$  manganite have been studied, using powder X-ray diffraction (XRD), transmission electron microscope, field emission scanning electron microscope and magnetic measurements. The XRD refinement result indicates that both samples have rhombohedral structure. The micrometer-sized sample shows long-range ferromagnetic ordering with transition temperature,  $T_c \sim 225$  K. In a contrary, the temperature dependence of Ac susceptibility of nanometer-sized sample shows broad peak which is frequency dependent. The result of Ac susceptibility data for nanometer-sized sample revealed super-spin glass behavior for this sample at low temperatures. Also, the Dc magnetization measurements confirmed the superparamagnetic behavior of nanometer-sized sample at room temperature.

**Keywords:** Manganite, Ac susceptibility, super-spin glass

## 1. Introduction

Manganites  $\text{La}_{1-x}\text{A}_x\text{MnO}_3$  (A = Sr, Ca, Ba or vacancies) has created an enormous considerable interest due to the discovery of the so-called colossal magnetoresistance (CMR) and its applications as magnetic field sensors (Jin et al., 1994; Asamitsu et al., 1995; Zener, 1951). The properties of these compounds have been interpreted by double-exchange model (Zener, 1951) and Jahn-Teller distortion (Millis et al., 1995). By varying the composition  $x$ , and consequently tuning the  $\text{Mn}^{3+}/\text{Mn}^{4+}$  ratio, the compound  $\text{La}_{1-x}\text{A}_x\text{MnO}_3$  indicates various electrical, magnetic and structural behaviors. These behaviors were related to strong coupling among spin, charge, orbital degree of freedom and lattice vibrations.

It is well known that the magnetic properties of these materials strongly depend on the particle size (Sánchez et al., 1996; Zhang et al., 1997; Wang et al., 1999; Rostamnejadi et al., 2009; Daengsakul et al., 2012). Manganite nanoparticles display features like lower values of magnetization (Kameli et al., 2006), higher values of low field magnetoresistance (Kuberkar et al., 2012), exhibit superparamagnetic (SPM) phenomena (Rostamnejadi et al., 2012; Dormann et al., 1999) and etc. SPM nanoparticles with single domain microstructure have a high potential as carriers for biomedical applications (Pardhan et al., 2008; Thorat et al., 2013). Additionally the nanosize particles of manganites can have zero coercivity at room temperature, which are applicable for hyperthermia investigation.

In this work we have investigated the structural and magnetic behaviors of micrometer and nanometer-sized  $\text{La}_{0.9}\text{Sr}_{0.1}\text{MnO}_3$  (LSMO) manganite samples which are prepared by Microwave-assisted Sol-Gel grown. To the best of our knowledge this is a first report about the microwave synthesizing method for LSMO manganite samples.

## 2. Experimental

The LSMO nanometer and micrometer-sized manganite samples were synthesized by the microwave- assisted Sol-Gel method using a kitchen-type microwave furnace equipped with a 2.45 GHz generator with the output power of 1000 W. The appropriate amounts of  $\text{La}(\text{NO}_3)_3 \cdot 6\text{H}_2\text{O}$ ,  $\text{Mn}(\text{NO}_3)_2 \cdot 4\text{H}_2\text{O}$ , and  $\text{Sr}(\text{NO}_3)_2$  were dissolved in water and mixed with ethylene glycol and citric acid, forming a stable solution. The solution was then kept in a microwave furnace with 60% of output power. The obtained powder is calcined at 450 °C for 6 h. Sample S1 and sample S2 were obtained by annealing the powder at 575 °C and 1200 °C for 6 h, respectively, to obtain powders

with nanometer and micrometer-sized particles.

The synthesized samples were characterized by X-ray diffraction (XRD) using Cu K $\alpha$  radiation source. The morphology of the samples was determined by transmission electron microscopy (TEM) and field emission scanning electron microscopy (FESEM). The dynamic magnetic properties have been characterized by using Ac susceptometer (Lake Shore Ac susceptometer model 7000). The Dc magnetization of the samples were measured at room temperature on a vibrating sample magnetometer (VSM, model Meghnatis DaghighKavir).

### 3. Results and Discussion

#### 3.1 Structural Characterization

The XRD patterns of the samples (S1 (a) and S2 (b)) are shown in Figure 1. The XRD data is analyzed with Rietveld refinement using FULLPROF program (Carvajal et al., 1993). It is found that the samples are single phase with the rhombohedral structure (R-3c space group) and there is a good agreement between the experimental and calculated patterns. The estimated average lattice parameters are  $a = b = 5.511 \text{ \AA}$  and  $c = 13.352 \text{ \AA}$  which are found close agreement with reported values (Shinde et al., 2011).

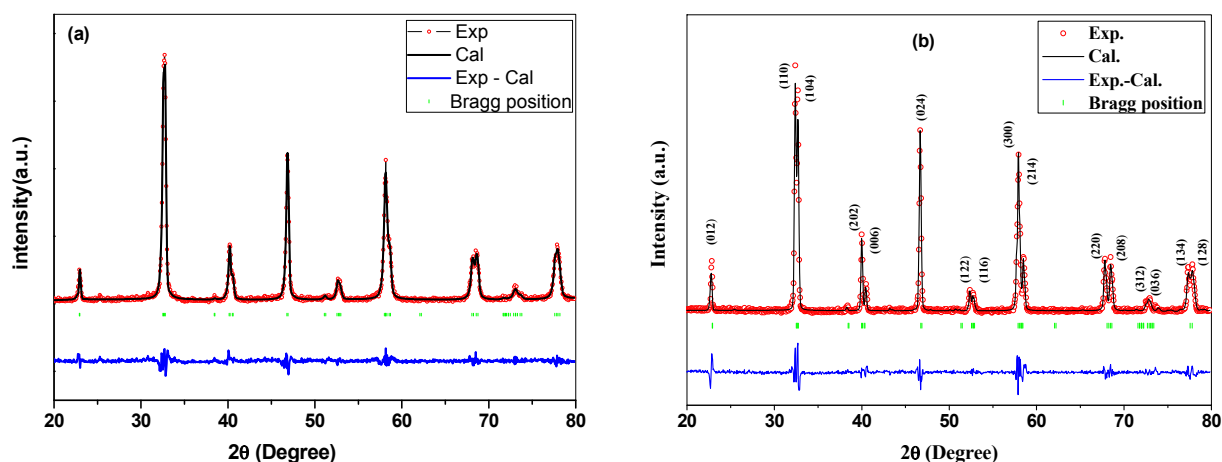


Figure 1. The observed and calculated (Rietveld analysis) XRD patterns of samples (a) S1 and (b) S2 at room temperature

The TEM micrograph of sample S1 and FESEM picture of sample S2 are shown in Figure 2. TEM micrograph shows that the mean particle sizes of the S1 sample is about 50 nm. Also, the selected area diffraction patterns of sample S1 confirms the crystalline nature of this sample. FESEM image of sample S2 indicates that the average particle size of the sample S2 is about one micrometer.

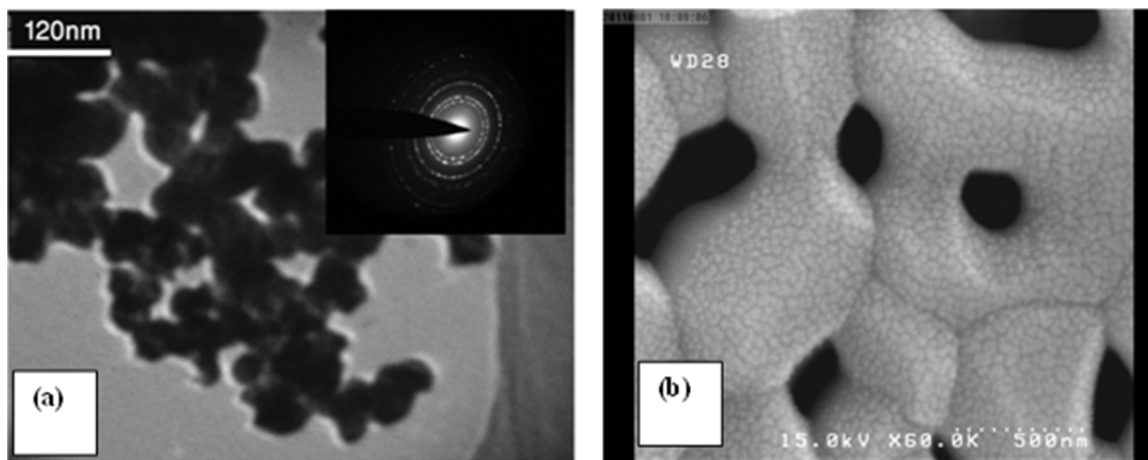


Figure 2. (a) TEM micrograph of sample S1, (b) FESEM picture of sample S2

### 3.2 Magnetic Characterization

Figure 3 shows temperature dependence of Ac susceptibility measurements (real part) for S1 and S2 samples in an Ac field of 1 mT and frequency of 333 Hz. The micrometer-sized sample shows long-range ferromagnetic (FM) ordering with transition temperature,  $T_c \sim 225$  K. In a contrary, the temperature dependence of Ac susceptibility of nanometer-sized sample shows broad peak which is frequency dependent (see Figure 4). This peak is normally related to the existence of SPM/spin glass behavior in magnetic systems (Dormann et al., 1997; Suzuki et al., 2009; Aslibeiki et al., 2012). The peak temperature corresponds to the average blocking temperature ( $T_B$ ) of the nanoparticles. Also, the magnitude of susceptibility of nanometer-sized sample is less than the micrometer-sized sample due to the spin disorders at surface of nanoparticles and presence of SPM behavior in this sample (Millis, 1998).

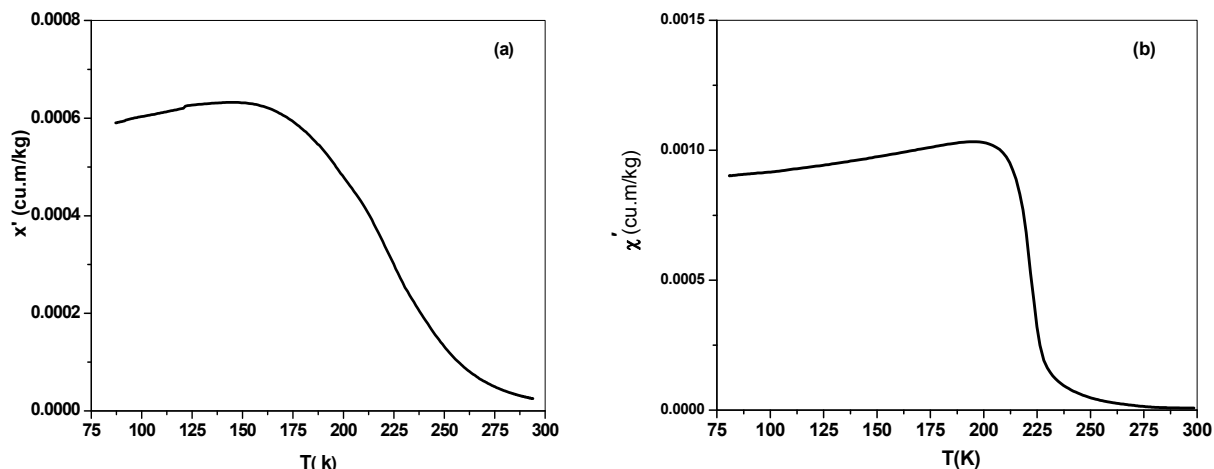


Figure 3. Temperature dependence of Ac magnetic susceptibility (real part) for (a) S1 and (b) S2 samples

To study the dynamic behavior of samples, frequency dependence of Ac susceptibility was measured on sample S1. Figure 4 shows the Ac susceptibility of sample S1 in an Ac field of 1 mT and frequency range of 33–1000 Hz. It is evident that the blocking temperature shifts to higher temperature as the frequency increases. In the non-interacting system, the frequency dependence of  $T_B$  obeys the Néel-Brown law (Tadic et al., 2012):

$$\tau = \tau_0 \exp(E_B/k_B T_B) \quad (1)$$

Where  $\tau$  is related to measuring frequency ( $\tau = 1/f$ ) and  $\tau_0$  is the magnetic moment flip time,  $k_B$  is the Boltzmann's constant and  $E_B$  is the energy barrier of the nanoparticles. When the energy of the barrier is less than thermal energy, the particles show SPM relaxation. Below  $T_B$  the magnetization of each nanoparticle is blocked along their easy anisotropy axes. Figure 5 shows the plot of  $\ln(f)$  versus  $1/T_B$ .

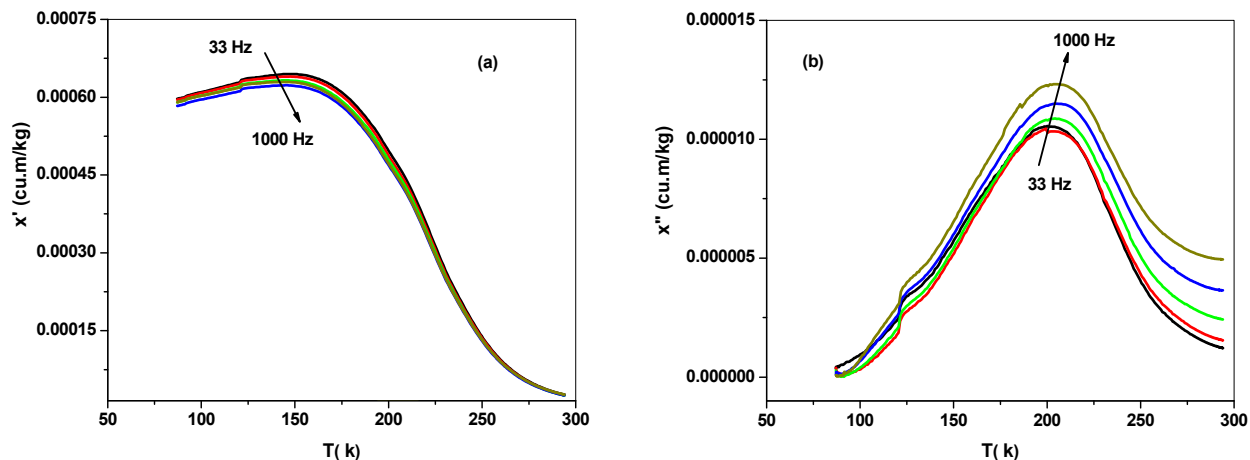


Figure 4. Frequency dependence of real (a) and imaginary (b) parts of Ac susceptibility for sample S1, in frequencies of 33–1000 Hz and ac field of 1 mT

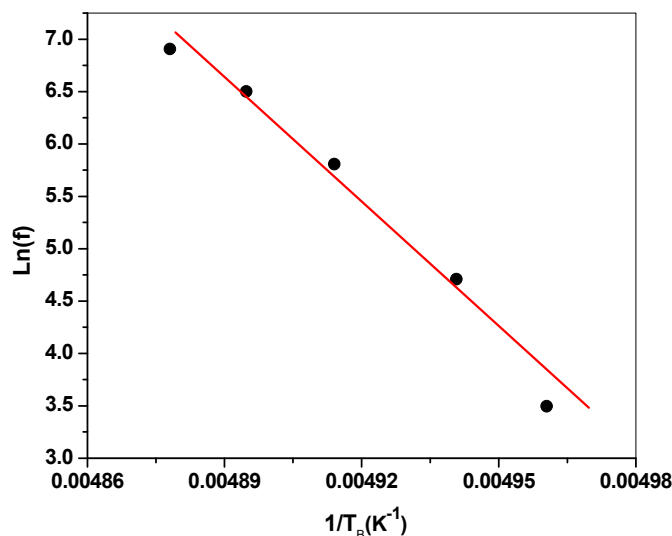


Figure 5. The best fits of Ac magnetic susceptibility data for sample S1, using Néel-Brown model

The value of  $\tau_0 \sim 1.26 \times 10^{-90}$  was estimated from data, were too small in comparison to the values of  $10^{-9} - 10^{-13}$  for SPM systems. As expected, this result simply indicates that there exists strong interaction between nanoparticles and the modified model is required to analysis the data. The Vogel-Fulcher law with an additional parameter  $T_0$  could be an appropriate model to describe the behavior of nanoparticles with medium interaction (Dormann et al., 1999),

$$\tau = \tau_0 \exp[E_B/k_B(T_B - T_0)] \quad (2)$$

Figure 6 shows the results of the fit with the Vogel-Fulcher law. It is well known that the Vogel-Fulcher law is valid only if  $T_0 \ll T_B$  (Dormann et al., 1999). The estimated value of  $T_0$  for S1 sample is about 199 K which is comparable with the average value of  $T_B$ ,  $\sim 202$  K. Therefore, the Vogel-Fulcher law cannot explain the behavior of sample.

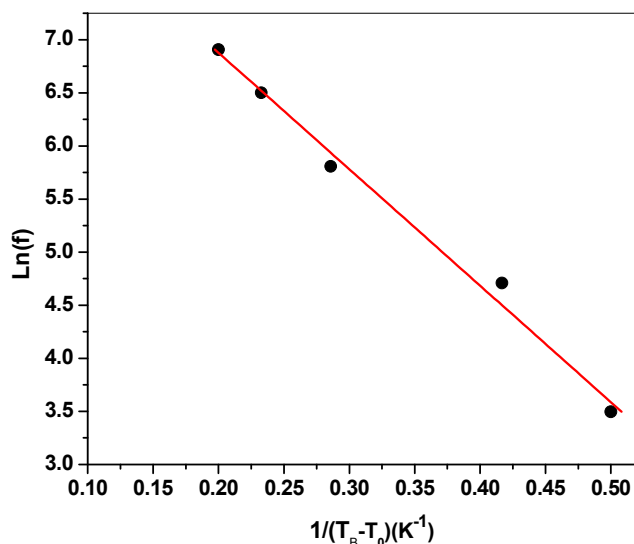


Figure 6. The best fits of ac magnetic susceptibility data for sample S1, using Vogel-Fulcher model

In the case of strong interaction between nanoparticles, magnetic nanoparticles indicate super-spin glass behavior (Aslibeiki et al., 2010). Critical slowing down model as a useful model has widely used to study the possibility of presence of a spin-glass (SG) behavior. This model is given as (Mydosh et al., 1996):

$$\tau = \tau_0 [(T_f/T_0) - 1]^{-z_0} \quad (3)$$

Where  $T_f$  is peak temperature in  $\chi''$  component of Ac susceptibility,  $T_0$  corresponds to DC value of  $T_f$  for  $f \rightarrow 0$ .  $\nu$  is the critical exponent of correlation length and  $z$  is a dynamic critical exponent (Mydosh et al., 1996; Thatar et al., 2009). From the best fits of this model (Figure 7),  $\tau_0$  was estimated as  $4.17 \times 10^{-11}$  and  $z\nu$  value as 4.8, which were in the predicted range for SG systems. This kind of SG behavior has been reported for interacting nanoparticles of  $\gamma\text{-Fe}_2\text{O}_3$  (Fiorani et al., 2002) and  $\text{Mn}_{0.5}\text{Zn}_{0.5}\text{Fe}_2\text{O}_4$  ferrite nanoparticles (Parekh et al., 2010). Since each particle contains  $10^3\text{--}10^4$  atoms (spin), this behavior for interacting nanoparticles is called super-spin-glass behavior. It should be noted that the generated heat by nanoparticles in hyperthermia based therapy method is dependent on interactions between nanoparticles (Rahimi et al., 2013).

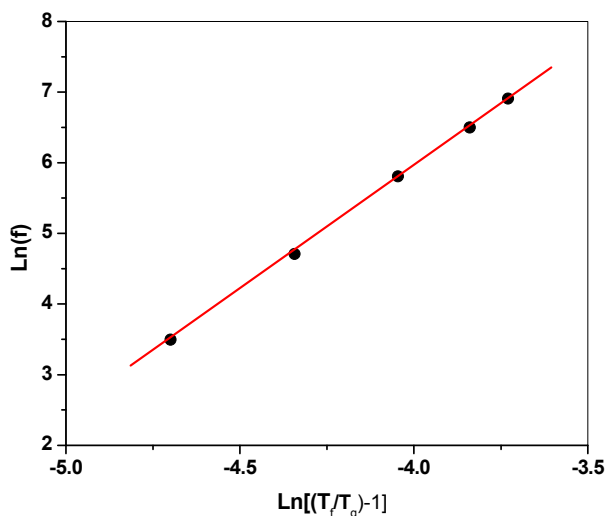


Figure 7. The best fits of ac magnetic susceptibility data for sample S1, using Critical slowing down model

The room temperature hysteresis loop of sample S1 is shown in Figure 8. Since the size of this sample is within the single domain limits the coercivity of this sample is zero and it shows SPM behavior at room temperature.

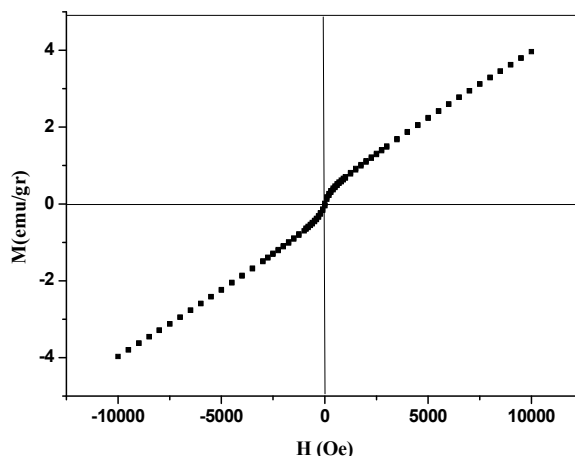


Figure 8. The room temperature Magnetization vs. magnetic field for sample S1

#### 4. Conclusions

The  $\text{La}_{0.9}\text{Sr}_{0.1}\text{MnO}_3$  nanometer and micrometer-sized manganite samples could be synthesized successfully by the Microwave-assisted Sol-Gel auto-combustion method. The micrometer-sized sample shows long-range ferromagnetic ordering. The zero coercivity and non-saturated magnetization show SPM behavior for the nano-sized sample at room temperature. It was found that the nanometer-sized sample has super-spin-glass

behavior with strongly interacting super-spins at low temperatures.

### Acknowledgments

The authors would like to thank the Payame Noor University for supporting this work.

### References

- Asamitsu, A., Moritomo, Y., Tomika, Y., Arima T., & Tokura, Y. (1995). A structural phase transition induced by an external magnetic field. *Nature*, 373, 407-409. <http://dx.doi.org/10.1038/373407a0>
- Aslibeiki, B., Kameli, P., Manouchehri, I., & Salamati, H. (2012). Strongly interacting superspins in Fe<sub>3</sub>O<sub>4</sub> nanoparticles. *Current Applied Physics*, 12(3), 812-816. <http://dx.doi.org/10.1016/j.cap.2011.11.012>
- Aslibeiki, B., Kameli, P., Salamati, H., Eshraghi, M., & Tahmasebi, T. (2010). Superspin glass state in MnFe<sub>2</sub>O<sub>4</sub> nanoparticles. *Journal of Magnetism and Magnetic Materials*, 322(19), 2929-2934. <http://dx.doi.org/10.1016/j.jmmm.2010.05.007>
- Carvajal, J. R. (1993). Recent advances in magnetic structure determination by neutron powder diffraction. *Physica B: Condensed Matter*, 192(1-2), 55-69. [http://dx.doi.org/10.1016/0921-4526\(93\)90108-I](http://dx.doi.org/10.1016/0921-4526(93)90108-I)
- Daengsakul, S., Thomas, C., Mongkolkachit, C., & Maensiri, S. (2012). Effects of crystallite size on magnetic properties of thermal-hydro decomposition prepared La<sub>1-x</sub>Sr<sub>x</sub>MnO<sub>3</sub> nanocrystalline powders. *Solid State Sciences*, 14(9), 1306-1314. <http://dx.doi.org/10.1016/j.solidstatesciences.2012.07.009>
- Dormann, J. L., Fiorani, D., & Tronc, E. (1997). Magnetic Relaxation in Fine-Particle Systems. *Advances in Chemical Physics*, 98, 283. <http://dx.doi.org/10.1002/9780470141571.ch4>
- Dormann, J. L., Fiorani, D., & Tronc, E. (1999). On the models for interparticle interactions in nanoparticle assemblies: comparison with experimental results. *Journal of Magnetism and Magnetic Materials*, 202(1), 251-267. [http://dx.doi.org/10.1016/S0304-8853\(98\)00627-1](http://dx.doi.org/10.1016/S0304-8853(98)00627-1)
- Fiorani, D., Testa, A., Lucari, F., D'orazio, F., & Romero, H. (2002). Magnetic properties of maghemite nanoparticle systems: surface anisotropy and interparticle interaction effects. *Physica B: Condensed Matter*, 320(1-4), 122-126. [http://dx.doi.org/10.1016/S0921-4526\(02\)00659-2](http://dx.doi.org/10.1016/S0921-4526(02)00659-2)
- Jin, S., Tiefel, T. H., MacCormack, M., Fastnacht, R. A. Ramesh, R., & Chen, L. H. (1994). Thousandfold change in resistivity in magnetoresistive La-Ca-Mn-O films. *Science*, 264(5157), 413-415. <http://dx.doi.org/10.1126/science.264.5157.413>
- Kameli, P., Salamati, H., & Aezami, A. (2006). Effect of particle size on the structural and magnetic properties of La<sub>0.8</sub>Sr<sub>0.2</sub>MnO<sub>3</sub>. *Journal of Applied Physics*, 100(5), 053914. <http://dx.doi.org/10.1063/1.2345036>
- Kuberkar, D. G., Doshi, R. R., Solanki, P. S., Khachar, U., Vagadia, M., Ravalia, A., & Ganesan, V. (2012). Grain morphology and size disorder effect on the transport and magnetotransport in Sol-Gel grown nanostructured manganites. *Applied Surface Science*, 258(22), 9041-9046. <http://dx.doi.org/10.1016/j.apsusc.2012.05.149>
- Millis, A. J. (1998). Lattice effects in magnetoresistive manganese perovskites. *Nature*, 392, 147-150. <http://dx.doi.org/10.1038/32348>
- Millis, A. J., Littlewood, P. B., & Shramin, B. I. (1995). Double exchange alone does not explain the resistivity of La<sub>1-x</sub>Sr<sub>x</sub>MnO<sub>3</sub>. *Phys. Rev. Lett.*, 74(25), 5144-5147. <http://dx.doi.org/10.1103/PhysRevLett.74.5144>
- Mydosh, J. (1996). Disordered magnetism and spin glasses. *Journal of Magnetism and Magnetic Materials*, 157-158, 606-610. [http://dx.doi.org/10.1016/0304-8853\(95\)01272-9](http://dx.doi.org/10.1016/0304-8853(95)01272-9)
- Parekh, K., & Upadhyay, R. J. (2010). Static and dynamic magnetic properties of monodispersed Mn<sub>0.5</sub>Zn<sub>0.5</sub>Fe<sub>2</sub>O<sub>4</sub> nanomagnetic particles. *Journal of Applied Physics*, 107(5), 053907. <http://dx.doi.org/10.1063/1.3310807>
- Pradhan, A. K., Bah, R., Konda, R. B., Mundle, R., Mustafa, H., Bamiduro, O., ... Sellmyer, D. J. (2008). Synthesis and magnetic characterizations of manganite-based composite nanoparticles for biomedical applications. *Journal of Applied Physics*, 103(7), 07F704. <http://dx.doi.org/10.1063/1.2829906>
- Rahimi, M., Kameli, P., Ranjbar, M., Hajhashemi, H., & Salamati, H. (2013). The effect of zinc doping on the structural and magnetic properties of Ni<sub>1-x</sub>Zn<sub>x</sub>Fe<sub>2</sub>O<sub>4</sub>. *Journal of Materials Science*, 48(7), 2969-2976. <http://dx.doi.org/10.1007/s10853-012-7074-y>
- Rostamnejadi, A., Salamati, H., & Kameli, P. (2012). Magnetic Properties of Interacting La<sub>0.67</sub>Sr<sub>0.33</sub>MnO<sub>3</sub>

- Nanoparticles. *Journal of Superconductivity and Novel Magnetism*, 25(4), 1123-1132. <http://dx.doi.org/10.1007/s10948-011-1378-z>
- Rostamnejadi, A., Salamati, H., Kameli, P., & Ahmadvand, H. (2009). Superparamagnetic behavior of  $\text{La}_{0.67}\text{Sr}_{0.33}\text{MnO}_3$  nanoparticles prepared via sol-gel method. *Journal of Magnetism and Magnetic Materials*, 321(19), 3126-3131. <http://dx.doi.org/10.1016/j.jmmm.2009.05.035>
- Sánchez, R. D., Rivas, J., Vázquez, C., López-Quintela, A., Causa, M. T., Tovar, M., & Oseroff, S. (1996). Giant magnetoresistance in fine particle of  $\text{La}_{0.67}\text{Ca}_{0.33}\text{MnO}_3$  synthesized at low temperatures. *Applied Physics Letters*, 68(1), 134. <http://dx.doi.org/10.1063/1.116780>
- Shinde, K. P., Pawar, S. S., & Pawar, S. H. (2011). Influence of annealing temperature on morphological and magnetic properties of  $\text{La}_{0.9}\text{Sr}_{0.1}\text{MnO}_3$ . *Applied Surface Science*, 257(23), 9996-9999. <http://dx.doi.org/10.1016/j.apsusc.2011.06.126>
- Suzuki, M., Fullem, S. I., Suzuki, I. S., Wang, L., & Zhong, C. (2009). Observation of superspin-glass behavior in  $\text{Fe}_3\text{O}_4$  nanoparticles. *Phys. Rev. B.*, 79(2), 024418. <http://dx.doi.org/10.1103/PhysRevB.79.024418>
- Thakur, M., Patra, M., Majumdar, S., & Giri, S. (2009). Coexistence of superparamagnetic and superspin glass behaviors in  $\text{Co}_{50}\text{Ni}_{50}$  nanoparticles embedded in the amorphous  $\text{SiO}_2$  host. *Journal of Applied Physics*, 105(7), 073905. <http://dx.doi.org/10.1063/1.3103320>
- Thorat, N. D., Khot, V. M., Salunkhe, A. B., Prasad, A. I., Ningthoujam, R. S., & Pawar, S. H. (2013). Surface functionalized LSMO nanoparticles with improved colloidal stability for hyperthermia applications. *Journal of Physics D: Applied Physics*, 46(10), 105003. <http://dx.doi.org/10.1088/0022-3727/46/10/105003>
- Wang, K., Song, W., Yu, T., Zhao, B., Pu, M., & Sun, Y. (1999). Colossal magnetoresistance in fine particle of layered-perovskite  $\text{La}_{2-2x}\text{Ca}_{1+2x}\text{Mn}_2\text{O}_7$  ( $x = 0.3$ ) synthesized at low temperatures. *Physica Status Solidi (A)*, 171(2), 577-582. [http://dx.doi.org/10.1002/\(SICI\)1521-396X\(199902\)171:2<577::AID-PSSA577>3.0.CO;2-0](http://dx.doi.org/10.1002/(SICI)1521-396X(199902)171:2<577::AID-PSSA577>3.0.CO;2-0)
- Zener, C. (1951). Interaction between the d-shells in the transition metals. II. ferromagnetic compounds of manganese with perovskite structure. *Phys. Rev. B.*, 82(3), 403-405. <http://dx.doi.org/10.1103/PhysRev.82.403>
- Zhang, N., Ding, W., Zhong, W., Xing, D., & Du, Y. (1997). Tunnel-type giant magnetoresistance in the granular perovskite  $\text{La}_{0.85}\text{Sr}_{0.15}\text{MnO}_3$ . *Phys. Rev. B.*, 56(13), 8138-8142. <http://dx.doi.org/10.1103/PhysRevB.56.8138>

### Copyrights

Copyright for this article is retained by the author(s), with first publication rights granted to the journal.

This is an open-access article distributed under the terms and conditions of the Creative Commons Attribution license (<http://creativecommons.org/licenses/by/3.0/>).